Fabricating scaffolds by microfluidics

Kuo-yuan Chung,[1] Narayan Chandra Mishra,[2] Chen-chi Wang,[3] Feng-hui Lin,[4] and Keng-hui Lin[5,a)]
[1]*Institute of Physics, Academia Sinica, Taipei 115, Taiwan*
[2]*Department of Paper Technology, Indian Institute of Technology, Roorkee, Saharanpur 247 001, India*
[3]*Tzu Chi General Hospital, Taipei, Taiwan and Institute of Biomedical Engineering, National Taiwan University, Taipei 100, Taiwan*
[4]*Institute of Biomedical Engineering, National Taiwan University, Taipei 100, Taiwan*
[5]*Institute of Physics and Research Center for Applied Science, Academia Sinica, Taipei 115, Taiwan*

(Received 14 February 2009; accepted 27 March 2009; published online 21 April 2009)

In this paper, we demonstrate for the first time the technique to using microfluidics to fabricate tissue engineering scaffolds with uniform pore sizes. We investigate both the bubble generation of the microfluidic device and the application of foam as a tissue engineering scaffold. Our microfluidic device consists of two concentric tapered channels, which are made by micropipettes. Nitrogen gas and aqueous alginate solution with Pluronic® F127 surfactant are pumped through the inner and the outer channels, respectively. We observe rich dynamic patterns of bubbles encapsulated in the liquid droplets. The size of the bubble depends linearly on the gas pressure and inversely on the liquid flow rate. In addition, monodisperse bubbles self-assemble into crystalline structures. The liquid crystalline foams are further processed into open-cell solid foams. The novel foam gel was used as a scaffold to culture chondrocytes. © *2009 American Institute of Physics.*
[DOI: 10.1063/1.3122665]

I. INTRODUCTION

Tissue cells in the body grow in a three-dimensional (3D) mesh called an extracellular matrix. Nonetheless, the majority of *in vitro* cell cultures are performed on two-dimensional (2D) surfaces such as petri dishes and tissue culture flasks. 3D cell culture studies are performed in a wide variety of porous matrices, or scaffolds, which can support cell growth on or within their structures. To grow a functional tissue or organ, it is necessary to culture cells in three dimensions. Differences, such as different phenotypes, exist between cells grown in 2D or 3D cultures.[1–3] Conventional methods[4] for producing 3D scaffolds include freeze drying,[5] phase separation,[6] particle leaching,[7] electrospraying,[8] and electrospinning.[9] Scaffolds made by these methods have pores with a wide distribution in sizes and shapes, hence making it difficult to carry out systematic studies on the architectural influence of the differences in signaling, gene expression, and organization. To elucidate the effect on cell-to-cell and cell-to-matrix interactions due to structure, it is desirable to have highly ordered and uniform spatial structures. Moreover, scaffolds are often modified with bioactive molecules, such as growth factors, drugs, or adhesion peptides.[10,11] A more uniform spatial structure distributes the chemical stimuli more homogeneously.

Recently, several methods have been developed in fabricating 3D ordered scaffolds by solid freeform fabrication techniques[12] such as photolithographic patterning and layering,[13] direct writing,[14] and two-photon stereolithography.[15] Most methods involve expensive robotic control and time consuming pixel-by-pixel writing. Kotov *et al.*[16] adopted the self-assembly approach by

a)Electronic mail: khlin@phys.sinica.edu.tw.

templating colloidal crystals. Colloidal spheres were organized into crystals by slow evaporation of the solvent. The interstices were then infiltrated with scaffold materials. Finally, the colloidal spheres were removed by organic solvent or calcination. Scaffolds of inverted crystal structures are made. However, the removal step by calcination limits the scaffold materials, and the method that uses organic solvent is slow and harmful for cells with organic residues.

Scaffolds have been fabricated in the form of solid foam, which is formed by rapid solidification of liquid foam. Solid foams are classified into open-cell or closed cells foams depending on whether the cellular faces of its liquid parent are retained. Liquid foams are colloidal dispersions of gas bubbles in a liquid where the bubbles are in contact. They are thermodynamically metastable. Monodisperse foams self-assemble into crystalline phases and exhibit stronger mechanical strength and longer stability than polydisperse foams. Conventionally monodisperse foams consisting of 1–10 mm diameter bubbles are usually made by blowing gas through a liquid column. At this length scale, gravitational force drains the liquid significantly. Microfluidics, which manipulates fluidic flow on microscales, provides a new mean to generate monodisperse bubbles or droplets at the length scale of 100 μm. Foams of this length scale remain wet under gravity and are spontaneously and rapidly ordered.[17] They also fall into the regime of scaffold pores. Microfluidic methods that have been employed include flow focusing,[18,19] cross flowing,[20] and coflowing of liquid and gas streams.[21] The dynamics, mechanism, and scaling behaviors of bubble breakup are under intense investigation. In addition, rich, complex but repeating foam flows have also been reported.[22,23] There are also chaotic behaviors such as bifurcation which generates bidisperse bubbles.[18] For fundamental studies, the self-organized patterns of multiphasic fluidic flow in a simple microfluidic circuit provides an ideal testbed for studying self-organized dynamics in nonequilibrium conditions.[24] For application purposes, the multiphasic flow has been applied to fabricate new materials that encapsulate cells in small spherical closed cell foam.[25]

II. EXPERIMENTAL

A. Microfluidic device

Our microfluidic device was inspired by the work of Utada *et al.*[26] It was composed of two concentric micropipettes: One micropipette was made from a cylindrical capillary tube, nestled within the other which was made from a square capillary whose inner dimension was close to the outer diameter of the cylindrical tube (Fig. 1). The micropipettes were pulled by a micropipette puller (P-97, Sutter Instrument, USA). The bubbles were generated by injecting a filtered aqueous solution containing 1% alginate (Sigma, A2158) and 1% Pluronic® F127 surfactant through the outer channel and nitrogen gas through the inner channel. It has been shown that cells proliferate and maintain high viability at this concentration of Pluronic® F127.[27] The alginate solution was injected at a controlled flow rate by a syringe pump (Ph.D 22/2000, Harvard Apparatus, USA). The pressure was measured by a digital pressure indicator (PM, Heise, USA). After the flow parameters were adjusted, we waited for the system to reach a steady state before we took our measurement. The bubble formation process was imaged by an ultrahigh speed video camera (Phantom v4.2, Vision Research, USA). The exposure time was 10 μs and the images were captured in a reduced size 64×256 at 20 000 frames/s. The bubbles were collected in a petri dish and observed using a stereoscope (Leica EZ4, Switzerland).

B. Cell cultures

Articular cartilage sliced from porcine joints was incubated in Dulbecco's modified Eagle's medium (DMEM) containing 0.2% collagenase type II (Sigma) at 37 °C for 16 h. Chondrocytes, the matrix-forming cells of cartilage, used in this study were collected from a cartilage-digested solution and placed in a culture vessel, which was subsequently filled with the medium. The rotation speed of the centrifuge was set at 1500 rpm for 5 min. The cells subsequently collected were suspended in DMEM supplemented with 10% fetal bovine serum (Gibco) and 50 μg/ml vitamin C (Sigma). The cells were maintained in a humidified atmosphere of 5% CO_2 and 95% air at 37 °C, and the medium was replaced once every 3 days until the cells reached a confluent

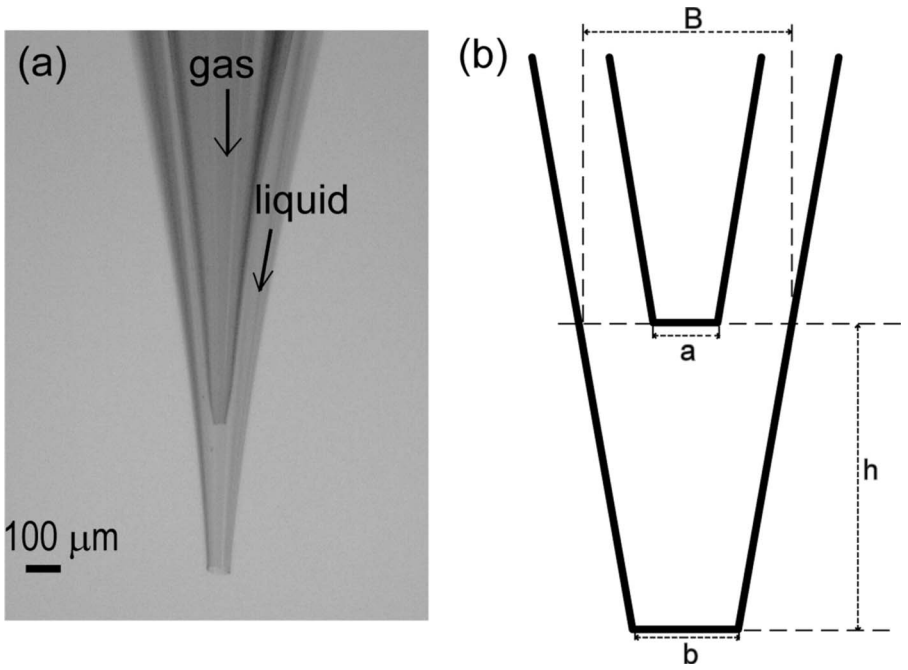

FIG. 1. (a) Optical image and (b) schematic drawing of the microfluidic device. The typical dimensions of devices are as follows: The diameter of the inner orifice, $a=25-35$ μm; the diameter of the outer orifice, $b=60-75$ μm; the tip-to-tip distance, $h=350-450$ μm; and the diameter of the base, $B=350-450$ μm.

population ($\geq 10^6$ cells) on 100 mm culture dishes. After the scaffolds were twice rinsed with the culture medium in 12-well culture plates, the cells were injected into the alginate scaffolds. The culture medium was then added to scaffold-containing well. 100 units/ml penicillin and 100 μg/ml streptomycin were added to prevent bacteria growth. The plates were transferred to an incubator at 37 °C with 5% CO_2, and their media were changed once every 2 days.

III. RESULTS

A. Bubble generation

Bubble formation occurred at the cavity between the inner orifice and the outer orifice of the microfluidic device. The gas stream expanded at the exit of the inner orifice, constricting the passage of the fluid flow, and eventually breaking up into bubbles. The liquid flow containing bubbles inside changed from jetting to dripping when the liquid flow rate was decreased, as shown in Fig. 2 and videos of the processes are available (enhanced). The liquid bridge between the bubbles became thinner and shorter and eventually disappeared. The very thin filamentlike bridge is the characteristic of viscoelastic fluid flow. At low liquid flow rates, there was an inadequacy of surrounding liquid to stabilize the bubble [Fig. 2(d)]. Bubbles burst at the exit of the outer orifice. There were times that all the large bubbles were all broken during the process and only the small bubbles survived inside the smaller liquid droplets [Fig. 2(e)].

The gas pressure P and liquid flow rate Q_L determined the size of the bubbles and the liquid droplets coming from the outer orifice. The combination of patterns of bubbles enclosed in the liquid streams were rich, ranging from "periodic droplets containing bubbles" to "pearls in a thread," and even "foam ribbons" [Figs. 3(b)–3(d)] and selected videos of these processes are available (enhanced). A representative state diagram of the patterns is shown in Fig. 3. When the gas pressure was not high enough to overcome the shear stress exerted by the outer fluid flow, there was only liquid flow. As the gas pressure is increased over a critical point (P_0), single monodisperse bubbles flow out in a liquid jet. P_0 increases linearly with the liquid flow rate. When the liquid flow rate was lower and the gas pressure was higher, bidisperse bubbles were generated

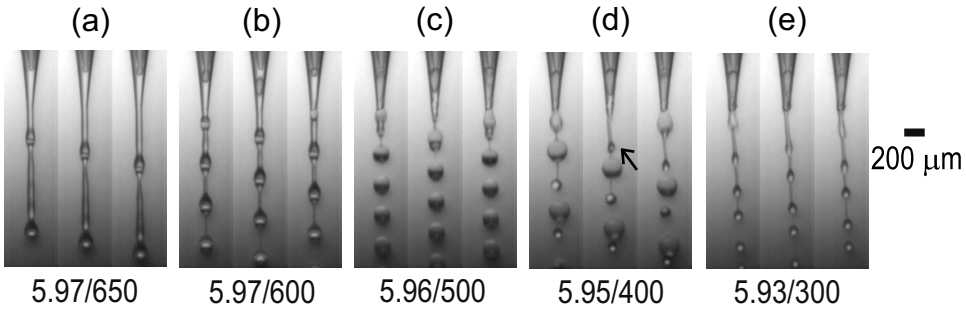

FIG. 2. Morphology of liquid droplets containing bubbles at a constant pressure and decreased flow rate, denoted as pressure (psi)/flow rate (/min) at the bottom of each image: (a) A jet, (b) a thinning jet, (c) monodisperse droplets, (d) bidisperse droplets, and (e) only small droplets. The arrow indicates a burst bubble. Videos of the processes are available (enhanced). [URL: http://dx.doi.org/10.1063/1.3122665.1]

and encapsulated as a pair of large and small bubbles within a liquid droplet. The formation of small bubbles was too fast to be captured by the camera but their existence was confirmed by examining the collected bubbles [Fig. 3(e.1)]. At even lower fluid flow rates or higher gas pressures, the bubbles became unstable in liquid droplets and bursted in the air. The states of the monodisperse bubbles were re-entrant, though many of the bubbles burst in the flight of air. In the region where the bubbles were unstable, there existed bubbles in bidisperse or polydisperse states. In general, the bubbles were less stable and more polydisperse at a low liquid flow rate and high gas pressure.

We measured the diameters of the bubbles from the monodisperse states and from the large bubbles from the bidisperse and the burst state. Figure 4 shows that the curves of the bubble diameter D_b increased linearly with P and plateaued at very high P. D_b was inversely proportional to Q_L below the plateau. When P was normalized by the onset pressure P_0, the diameter of the bubble depended only on the ratio of P/P_0 and P_0 is proportional to Q_L. The plateau of the bubble diameters was due to the constrained cavity whose dimensions of the shown microfluidic device were $b=62\ \mu$m, $h=413\ \mu$m, and $B=130\ \mu$m. The equivalent spherical diameter with the same cavity volume was $181\ \mu$m, which correlated well with our experimental data where the plateau was approximately $172\ \mu$m. Different microfluidic devices gave similar state diagrams and the same scaling of bubble diameter to the pressure.

B. Scaffolds

We collected bubbles from the monodisperse state and high in gas fraction. They spontaneously self-assembled into crystalline foam structures spontaneously and were stable for several minutes. When collected, the liquid foam is collected about 3 mm in thickness in a 3 cm petri dish. A 100 mM or higher $CaCl_2$ solution was added quickly and continuously for a few minutes to cross-link the alginate. Incomplete gelation occurred when the liquid foam was too thick due to the limit of ion diffusion. The cross-linked solid foam was placed in liquid and degassed under vacuum until the pores were filled with water. The pressure difference between the bubbles and the ambient atmosphere ruptured the film between the bubbles and only plateau borders were left. A sliced cross-linked open-cell foam scaffold was observed under an environmental scanning electron microscope (SEM) [FEI Quanta 2000, Fig. 5(a)]. Fluorescent microspheres were incorporated into the alginate solution for the observation by the Leica TCS SP5 confocal microscope shown in Fig. 5(b). Both figures show highly ordered and interconnected pores of scaffolds. The ordered honeycomb structure was more pronounced near the surfaces of the scaffold. Deep inside the scaffold, the size distribution of the pores became broader but was still quite narrow compared to traditional alginate sponge. The spatial distribution of the pores was also less ordered. We believe that flowing calcium solution into alginate foam and the nonuniform gelation affected crystalline structures and the monodispersity of liquid foams. Nevertheless, the pores of scaffolds made by

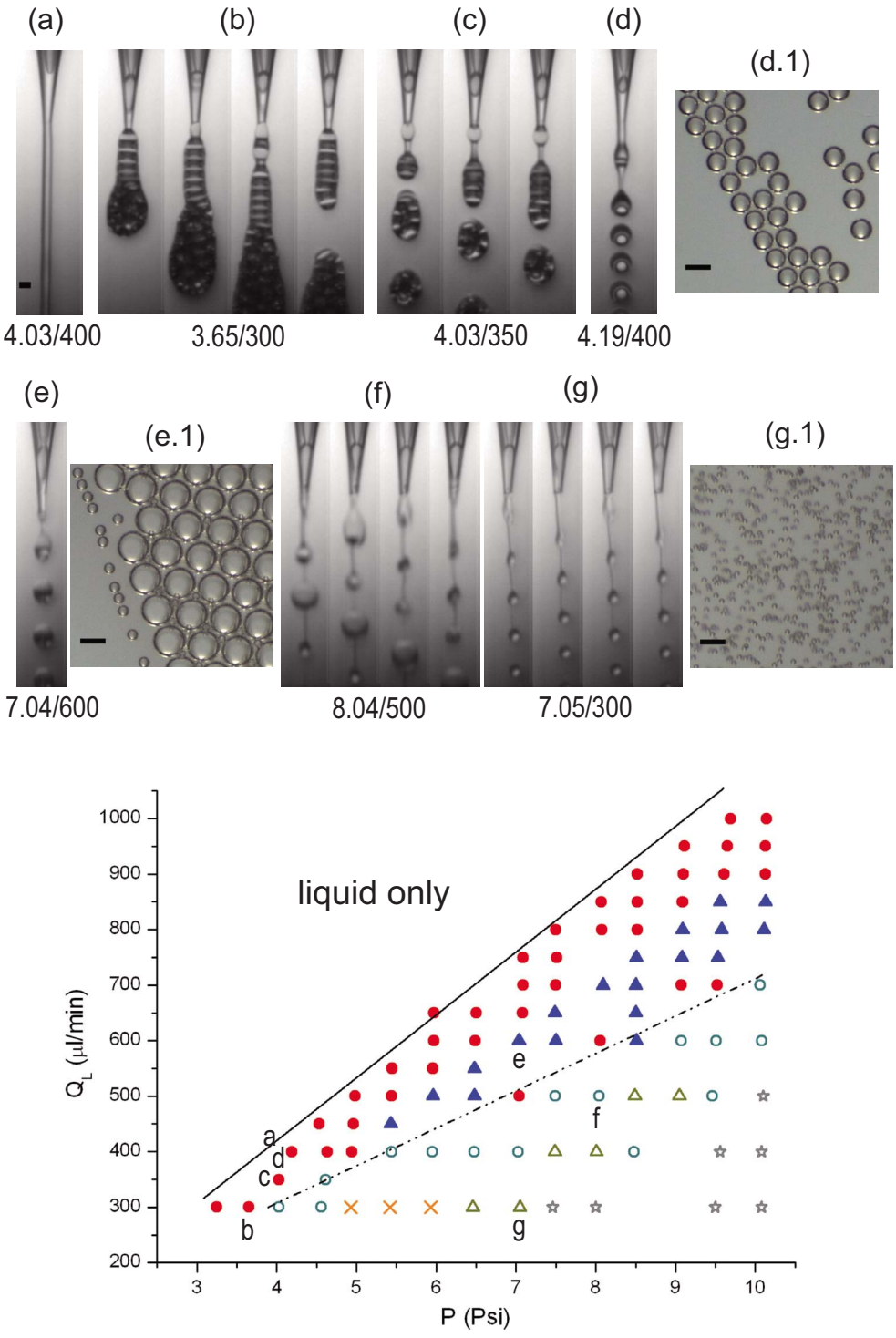

FIG. 3. Patterns of bubbles in liquid droplets at the exit of the device at different gas pressures (psi)/liquid flow rate (/min) and the corresponding state diagram of the Q_L and P and bubble morphology. The patterns include (a) no bubbles (water jet), [(b) and (c)] continuous bubble stream, (d) discontinued single bubbles, (e) bidisperse bubbles, (f) broken bubbles, and (g) tiny bubbles only. Photographs (d.1), (e.1), and (g.1) are optical images of collected bubbles corresponding to (d), (e), and (g), respectively. The solid line is used to draw the boundary where bubbles occur. The dashed line delineates the boundary where bubbles become unstable in droplets and break. The symbols describe monodisperse bubbles (solid/open circle), bidisperse bubbles (open/solid triangles), no bubbles (cross), and polydisperse bubbles (star). The open symbol denotes the occurrence of burst bubbles. All the scale bars shown here are 100 μm. Selected videos of these processes are available (enhanced). [URL: http://dx.doi.org/10.1063/1.3122665.2]

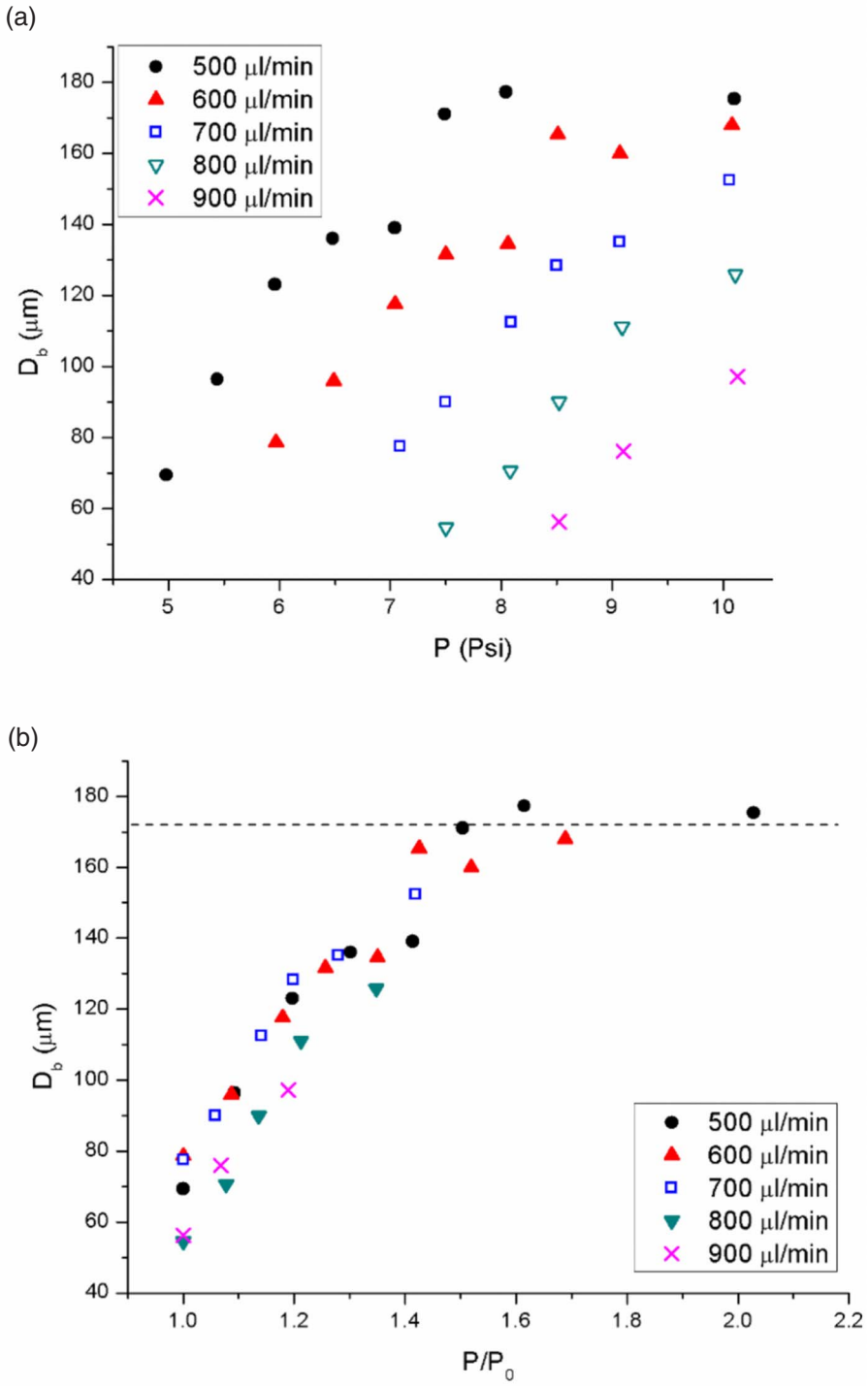

FIG. 4. Bubble diameter D_b measured at the atmospheric pressure is plotted against (a) P and (b) P/P_0 at different Q_L. The dashed line indicates a plateau of the maximum bubble diameters.

the microfluidic method were more controlled than the conventional sponge. We cultured chondrocytes on the hydrogel scaffolds. The cells were introduced into the scaffold by injection. The chondrocytes grew for more than a month in our scaffolds, and Figs. 5(c)–5(e) show their proliferation over time.

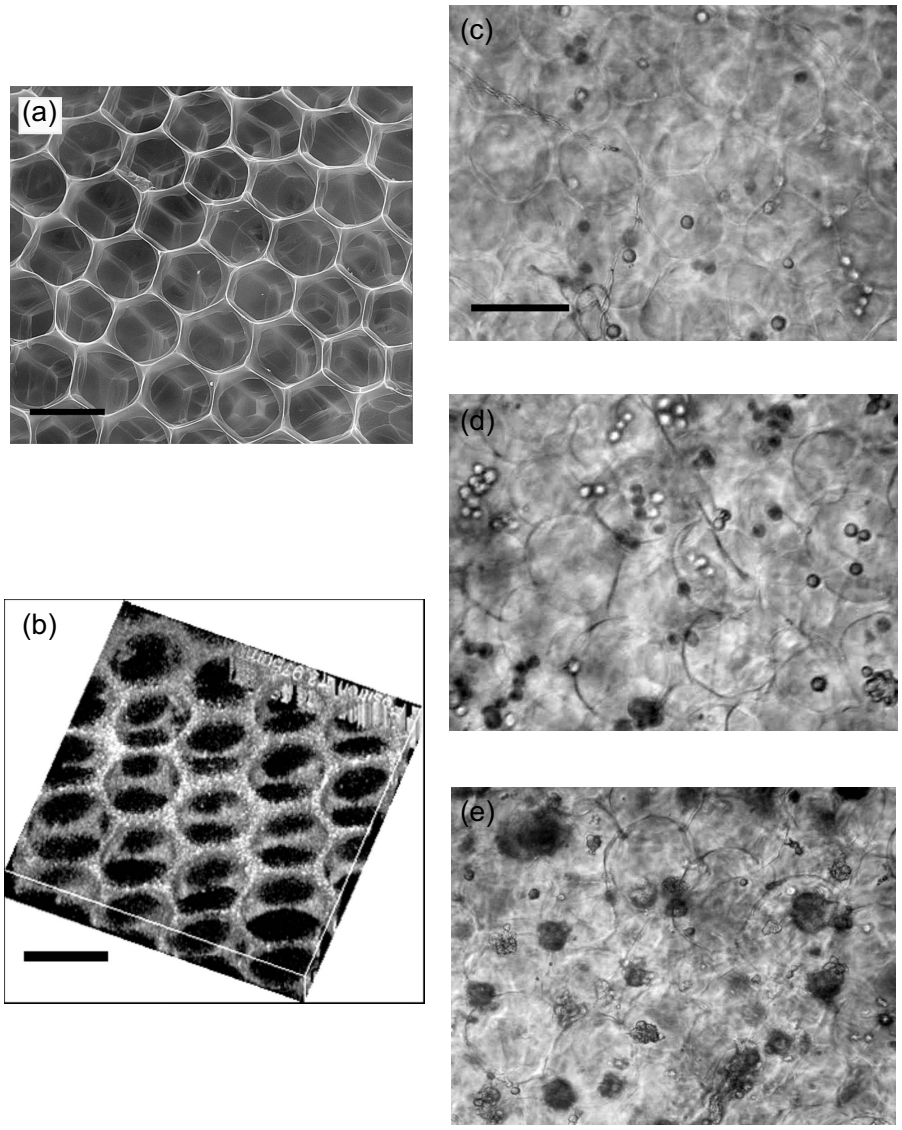

FIG. 5. (a) SEM image and (b) confocal image of the scaffold. The pores are highly ordered and interconnected. Chondrocytes cultured in a scaffold on (c) day 1, (d) day 3, and (e) day 7. The dark regions in (e) are clusters of cells. All the scale bars are 100 μm.

IV. CONCLUSIONS

Microfluidic technology continues to exert an impact on biological applications.[28] The ability to generate monodisperse droplets drives the development of cell-based assays in picoliter and large statistics.[29,30] In this paper, we demonstrated a further application for fabricating scaffolds of uniform pore size for tissue engineering and 3D cell cultures. This method is simple, fast, and inexpensive. We have shown that chondrocytes proliferate in the new scaffolds. Similar microenvironments are suitable for further studies of the effect of pore size and porosity in tissue engineering. The uniformity in pore size can be improved by increasing the stability of foam and by more controlled gelation process. This method can be used with other scaffold materials. Our new rigid axisymmetric coflow device was able to produce complex patterns. The peculiar structures of the droplets containing bubbles can be further engineered into new materials by polymerizing the liquid in the air. The mechanism of breakup and the governing law on patterns is under further

investigation. Our work not only shows the novel biological applications of microfluidic technology but also contributes to the current research trends of the biphasic flow and the dynamic patterning using the microfluidic device.

ACKNOWLEDGMENTS

We would like to thank our students and research assistants who have participated in this work in Keng-hui Lin's team. Chia-hung Chen helped in the fabrication of the microfluidic device. Yen-liang Liu and Hsiao-chao Chen helped in culturing chondrocytes. Jun-hung Pan took the confocal images. Wuen-shi Chen helped in the data analysis of the fluidic patterns. We thank Dr. Hsueh-chia Chang of the Department of Chemical Engineering, University of Notre Dame and Dr. Jih-chiang Tsai for their insight into fluidic flow. We also thank Professor Adam Hsieh and Professor John Fisher of the Department of Bioengineering, University of Maryland on suggestions about scaffolds. Support for this work was provided by Taiwan NSC under Grant No. 97-2112-M-001-016, the starting fund from the Institute of Physics and the nano-bio program of the Research Center for Applied Sciences, Academia Sinica, Taiwan.

[1] A. Abbott, Nature (London) **424**, 870 (2003).
[2] E. Cukierman, R. Pankov, D. R. Stevens, and K. M. Yamada, Science **294**, 1708 (2001).
[3] T. Sun, S. Jackson, J. W. Haycock, and S. MacNeil, J. Biotechnol. **122**, 372 (2006).
[4] *Methods of Tissue Engineering*, edited by A. Atala and R. P. Lanza (Academic, San Diego, 2002).
[5] S. Zmora, R. Glicklis, and S. Cohen, Biomaterials **23**, 4087 (2002).
[6] J. H. Aubert and R. L. Clough, Polymer **26**, 2047 (1985).
[7] A. G. Mikos, A. J. Thorsen, L. A. Czerwonka, Y. Bao, R. Langer, D. N. Winslow, and J. P. Vacanti, Polymer **35**, 1068 (1994).
[8] A. C. Sullivan and S. N. Jayasinghe, Biomicrofluidics **1**, 034103 (2007).
[9] W. J. Li, C. T. Laurencin, E. J. Caterson, R. S. Tuan, and F. K. Ko, J. Biomed. Mater. Res. **60**, 613 (2002).
[10] H. J. Chung and T. G. Park, Adv. Drug Delivery Rev. **59**, 249 (2007).
[11] J. A. Rowley, G. Madlambayan, and D. J. Mooney, Biomaterials **20**, 45 (1999).
[12] S. J. Hollister, Nature Mater. **5**, 590 (2006).
[13] D. Gallego, N. Ferrell, Y. Sun, and D. J. Hansford, Mater. Sci. Eng., C **28**, 353 (2008).
[14] J. L. Simon, S. Michna, J. A. Lewis, E. D. Rekow, V. P. Thompson, J. E. Smay, A. Yampolsky, J. R. Parsons, and J. L. Ricci, J. Biomed. Mater. Res. Part A **83A**, 747 (2007).
[15] M. S. Hahn, J. S. Miller, and J. L. West, Adv. Mater. (Weinheim, Ger.) **18**, 2679 (2006).
[16] N. A. Kotov, Y. F. Liu, S. P. Wang, C. Cumming, M. Eghtedari, G. Vargas, M. Motamedi, J. Nichols, and J. Cortiella, Langmuir **20**, 7887 (2004); Y. J. Zhang, S. P. Wang, M. Eghtedari, M. Motamedi, and N. A. Kotov, Adv. Funct. Mater. **15**, 725 (2005).
[17] M. Vignes-Adler and D. Weaire, Curr. Opin. Colloid Interface Sci. **13**, 141 (2008).
[18] P. Garstecki, M. J. Fuerstman, and G. M. Whitesides, Phys. Rev. Lett. **94**, 234502 (2005).
[19] E. Lorenceau, Y. Y. C. Sang, R. Hohler, and S. Cohen-Addad, Phys. Fluids **18**, 097103 (2006).
[20] P. Garstecki, M. J. Fuerstman, H. A. Stone, and G. M. Whitesides, Lab Chip **6**, 437 (2006).
[21] G. F. Christopher and S. L. Anna, J. Phys. D **40**, R319 (2007).
[22] P. Garstecki and G. M. Whitesides, Phys. Rev. Lett. **97**, 024503 (2006).
[23] J. P. Raven and P. Marmottant, Phys. Rev. Lett. **97**, 154501 (2006).
[24] A. M. Gañán-Calvo, Nat. Phys. **1**, 139 (2005).
[25] S. Arumuganathar, N. Suter, and S. N. Jayasinghe, Adv. Mater. (Weinheim, Ger.) **20**, 4419 (2008).
[26] A. S. Utada, E. Lorenceau, D. R. Link, P. D. Kaplan, H. A. Stone, and D. A. Weitz, Science **308**, 537 (2005).
[27] S. F. Khattak, S. R. Bhatia, and S. C. Roberts, Tissue Eng. **11**, 974 (2005).
[28] *Biological Applications of Microfluidics*, edited by F. A. Gomez (Wiley, New York, 2008).
[29] C. H. J. Schmitz, A. C. Rowat, S. Köster, and D. A. Weitz, Lab Chip **9**, 44 (2009).
[30] M. Y. He, J. S. Edgar, G. D. M. Jeffries, R. M. Lorenz, J. P. Shelby, and D. T. Chiu, Anal. Chem. **77**, 1539 (2005).